

Received June 27, 2019, accepted July 7, 2019, date of current version August 9, 2019.

Digital Object Identifier 10.1109/ACCESS.2019.2929690

A Soft-Robotic Approach to Anthropomorphic Robotic Hand Dexterity

JIANSHU ZHOU¹, (Student Member, IEEE), XIAOJIAO CHEN¹, (Student Member, IEEE), UKYOUNG CHANG¹, JUI-TING LU¹, CLARISSE CHING YAU LEUNG¹, YONGHUA CHEN¹, (Senior Member, IEEE), YONG HU², (Senior Member, IEEE), AND ZHENG WANG^{1,3}, (Senior Member, IEEE)

¹Department of Mechanical Engineering, The University of Hong Kong, Hong Kong

²Department of Orthopedics and Traumatology, Li Ka Shing Faculty of Medicine, The University of Hong Kong, Hong Kong

³Department of Mechanical and Energy Engineering, Southern University of Science and Technology, Shenzhen 518055, China

Corresponding author: Zheng Wang (zheng.wang@ieee.org)

This work was supported in part by Hong Kong RGC-GRF/ECS under Grant 27210315, in part by the Innovation and Technology Fund (ITF) under Grant ITS/140/18 and Grant IT457/17FP, in part by HKU Seed Funding under Grant 201611159196, Grant 201611160034, Grant 201711160023, and Grant 201711159158.

ABSTRACT Soft robotics is quickly emerging in anthropomorphic robotic hand design, with innovative soft robot hands reported to achieve a remarkably large subset of human hand dexterity, despite their substantially lower mechanistic sophistication compared to conventional rigid or underactuated robotic hands. More interestingly, soft robot hands were most successful in reproducing object grasping, rather than in-hand manipulation tasks. Inspired by this notable advance, this paper investigated the soft robotic approach, on the influence of passive compliance to functional dexterity, offering insights to their efficacy and addressing the remaining gaps to fully replicating human hand dexterous motions. A novel soft robotic hand, BCL-26, with 26 independent degrees of freedom was then proposed, replicating the human hand model. The BCL-26 hand achieved full scores in different aspects of functional dexterity measures, on GRASP taxonomy, thumb dexterity, and in-hand manipulation. Completed with proprietary actuation and control, the overall BCL-26 hand system facilitated further investigations from the influence of passive compliance achieving in-hand manipulation/writing, to fully independent control of all finger joints, and to metacarpal extension enabled by the soft robotic approach. The BCL-26 hand, as a new soft-robotic addition to mechanistically exact human hand replicas, had demonstrated the promising potentials of soft robotics, it also enabled investigating the dexterities of robotic and human hand.

INDEX TERMS Humanoid robotic hand, soft robotics, robot hand design and control.

I. INTRODUCTION

Hand dexterity is of tremendous value to humans for exploring and interacting with the world ([1], [2]). Replicating human hand dexterity has provided numerous insights on robotic hand/end-effector design for healthcare([3]–[8]), service ([9], [10]) & industry ([11]–[13]), and space applications ([14], [15]). The design of anthropomorphic robotic hands has taken highly diverse approaches ([16]–[18]): i) for kinematic resemblance of mechanical joints and links ([10], [19]–[22]); ii) for functional resemblance of human-hand functionalities using significantly simplified mechanisms, from mechanistic under-actuation

([5], [9], [13], [23]) to model reduction by virtual finger ([24], [25]), Synergies ([26], [27]), Eigengrasp ([28], [29]), and other approaches ([8], [30], [31]), for prosthetics or similar applications ([26], [32]); iii) for frontier exploration with new materials ([33]–[35]), actuation/control ([36]–[38]), and sensing modalities ([39]–[41]), achieving innovative object grasping functionalities at various levels ([16], [41], [42]).

Soft robotic hands are quickly emerging with novel soft structural ([33], [43], [44]), actuation ([45], [46]), and sensing ([39], [47], [48]) elements. Constructed from soft materials, fluid-driven soft robotic hands could achieve a list of distinctive features from rigid robotic hands, including inherent compliance ([35], [49]–[51]), integrated sensing ([47], [52]), and impact resistance ([49], [53]). Soft robotic hands offer excellent grasping dexterity ([54], [55]),

The associate editor coordinating the review of this manuscript and approving it for publication was Aysegul Ucar.

object adaptability ([35], [55], [56]), and passive safety ([49], [57]), with very compact and lightweight designs (with actuation and control hardware often located remotely) ([35], [37], [39], [55]), as well as smooth and compliant characteristics ([45], [58]).

However, the emergence of soft robotic hands also gave rise to new challenges and curiosities: abundant reported works on compliant and soft robotic hands have demonstrated that a very large subset (often 80%-90%) of the hand dexterity functionalities could be achieved by a significantly lower (30%-40%) DOF mechanism with strategically composed compliance ([9], [25], [35], [39]), while the complexity and speed requirements on actuation and control were also dramatically reduced using innovative approaches [59]. The overwhelming set of observations would inevitably lead to the introspection of revisiting the commonly-adopted DOF-approach and exploring new insights brought by the emerging soft-robotic approach to robotic hand design.

A. FUNCTIONAL-ORIENTED HAND DEXTERITY MEASURES

Mechanical Dexterity, often as *Dexterity* in robotics literature ([61]–[64]), involves both the mechanistic complexity and its functional potential, without explicitly considering other aspects such as sensory feedback and control of a robotic hand. The concept of dexterity in robotic hands predominantly concerns the resultant functional performance of the hand, which is described by the range of achievable grasping postures ([65]–[67]) and manipulations ([38], [68]). In this article, three highly distinctive measures of functional-oriented evaluation are adopted for a comprehensive assessment of hand dexterity:

- **Grasping taxonomy.** By grasping a list of benchmarking objects in specific postures, the grasping taxonomy provides a static assessment of the capability of the hand in object grasping, as proposed in [66] and the GRASP taxonomy [67]. This is a commonly adopted benchmark for robotic hands with 33 taxonomies [67].

- **Thumb dexterity** has always been of vital importance in various clinical aspects ([69], [70]). The widely acknowledged Kapandji test of 11 different hand postures (scores 0-10) using the thumb to touch different target regions of the hand [70]. Similar to the grasping taxonomies, Kapandji scores are also static postures.

- **(In-hand) Manipulation taxonomy.** With the hand fixed, manipulate the object in-grasp only by movements of the hand's thumb/fingers/palm. In-hand manipulation requires dynamic motions of objects, imposing higher requirements than the static postures. Commonly adopted manipulation taxonomy has 6 taxonomies, without considering relative motion between hand and object, corresponding to the 6-DOF general motion of a rigid body in space ([38], [68]).

B. SUMMARY OF MAIN CONTRIBUTIONS

Design, fabrication and control of a novel, anthropomorphic, 26-DOF soft-robotic hand BCL-26, being

the most dexterous soft robotic hand to-date, with human-hand-comparable mechanical dexterity. Two novel designs of soft-robotic joints were proposed to achieve substantially improved motion characteristics, spatial density, and control performances over state-of-the-art soft actuators. The prototyped BCL-26 hand could successfully complete **all 50 dexterity measures for the human hand** (33 GRASP taxonomies, 11 Kapandji tests, and 6 in-hand manipulation taxonomies), with 2kg maximum payload and a maximum spherical object size of 160mm in diameter.

Dexterity investigations on the BCL-26 dexterous soft robotic hand platform: i) understanding passive compliance through in-hand manipulation, including achieving in-hand writing for the first time in soft robotic hands, by; ii) intuitive human-hand direct mapping and control to BCL-26; iii) preliminary explorations on hyperextension, fully-independent finger joint control, and metacarpal extension.

II. DESIGN AND PROTOTYPING OF BCL-26 HAND

The design, modeling, and prototyping results of BCL-26 were highlighted in Figure 1. Taking an elastomeric-chamber, pneumatic-drive approach reported by many existing works on soft robotics ([35], [75], [52], [57]), the main novelties of the proposed design were the new V-chamber and X-chamber soft actuators, multi-chamber molding procedure, and the segmented design of the palm and the whole hand.

A. DESIGN OF NOVEL V-CHAMBER AND X-CHAMBER SOFT ACTUATORS

A prominent challenge for designing a soft robotic hand with high DOFs was the mismatch between the gradual bending motion of available soft actuators and the sharp, large-range bending in most human hand joints (CMC, IP, DIP, PIP, etc.). Further to this issue, the MCP joint for both the thumb and the fingers integrated 2 or more DOFs in one location, requiring for highly compact and large-range deformation in multiple directions.

To achieve joint-like bending motion with small bending radius and large bending range on soft robots, we proposed a **V-shape chamber** with the pinnacle of the V-chamber resembling the pivot point of an articulated joint in conventional mechanisms. Resulting of this chamber design, as shown in Figure 1(a), with a limiting layer to constrain axial elongation, the pinnacle of the V-chamber was the pivot point of bending, while the opening angle of the V-shape determined the range of bending and the pressure required. On the other hand, if two V-shape chambers were placed antagonistically without a limiting layer, forming an **X-chamber** actuator as shown in Figure 1(b), the segment would exhibit bilateral bending with the joint-pinnacle point as the center of articulation, as well as elongation when both chambers were inflated, resulting in 2-DOF motions for the entire segment. The proposed V- and X- chamber actuators substantially reduced the bending radius while increasing the bending range, enabling multiple actuators to be integrated into the confined space of the hand.

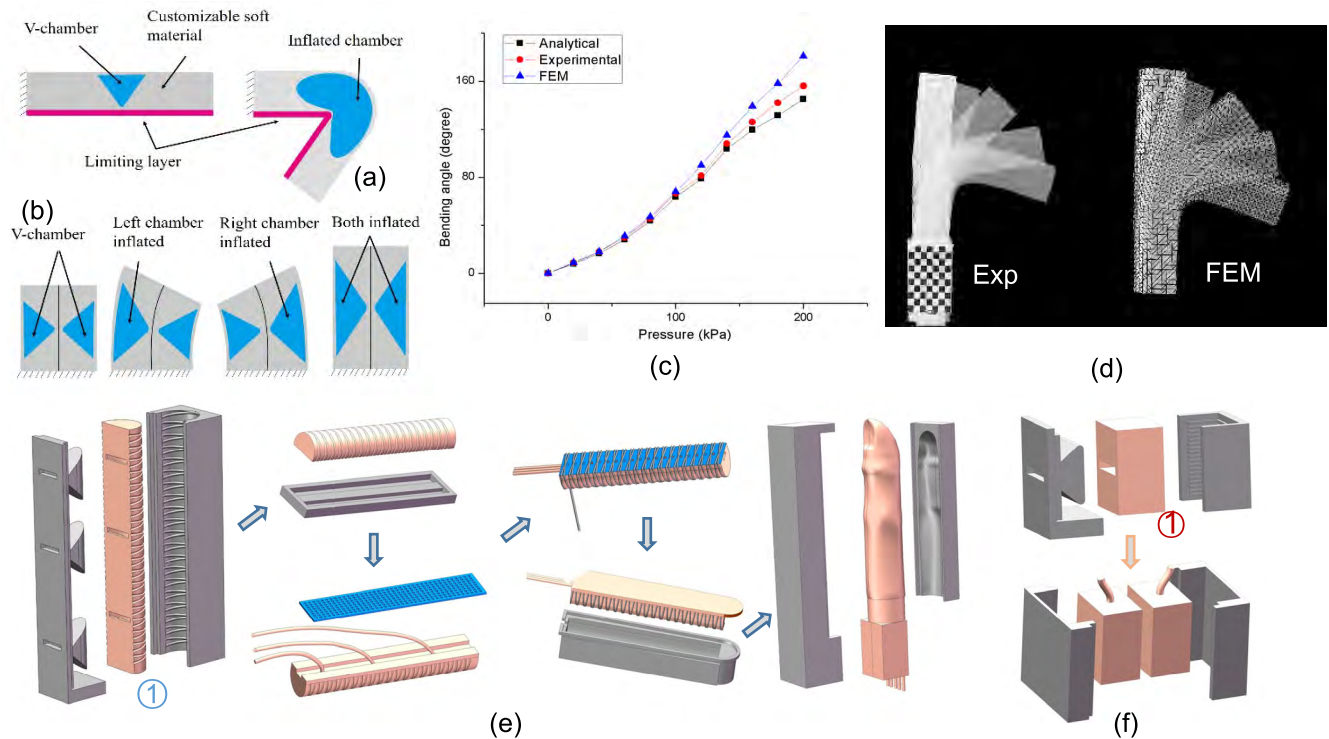


FIGURE 1. Design of novel soft robotic joints and fabrication of soft robotic fingers with 4-DOF. (a) V-chamber soft actuator; (b) X-chamber soft actuator; (c) comparison of analytical modeling and FEM results with experimental measures in bending angles; (d) comparison between FEM and experimental results at various bending angles; (e) multi-stage molding fabrication for the V-chamber actuator; (f) simplified molding from e) for Xchamber actuator.

A full parametric study with various design parameters on the V-chamber had been carried out to determine the optimal design for the BCL-26 design, including analytical modeling, Finite Element Modeling (FEM), and experimental prototyping. Results from the three approaches were in very good agreement (Figure 1(c, d)).

Fabrication and prototyping techniques were modified from the existing standard multi-stage molding for soft actuators ([45], [74]), because of the challenging high spatial density of the actuators on each finger. To address large bending range (large stretch ratio for the soft material chambers) and completely soft fingers (therefore no rigid auxiliary pneumatic fittings were allowed), two major modifications to the fabrication procedure were proposed: i) each chamber was molded reversely, with the pinnacle of the V-shape connecting to the base plate, both for the V-chamber and X-chamber designs (see molding stage 1 of Figure 1(e, f)), before attaching the bottom strain-limiting layer, allowing multiple chambers to be molded in one finger while reducing delamination risks during inflation (the seam at limiting layer underwent minimum stretch during chamber inflation); ii) flexible air tubing was embedded into each chamber at Stage (3) for V-shape, between the top and bottom layers before placing the straining limiting layer, so that in Stage (4) the encircling helical reinforcement wires could securely fasten the tubing into each chamber. Full details on the design, modeling, fabrication, and evaluation of the V- and X- actuators are included in the Supplementary Materials.

1) WHOLE HAND DESIGN WITH A SEGMENTED PALM

The surface of the human hand consists of three areas: the thumb, four fingers, and the palm Figure 2(a) [71]. The kinematic structure of the anatomical skeleton Figure 2(b) was often adopted by high-end robotic hands with high degrees of structural complexity ([11], [19], [21]). However, the palm surface area intersects with all 5 digits at MCP and CMC joints (Figure 2(c)), sub-dividing the palm into three “Functional Zones”: FZ-I for the thumb, FZ-II for the 4 fingers, and FZ-III for the palm (Figure 2(c)). In addition, the palm zone was further divided into 4 sub-zones (Figure 2(d)): **FZ-III-1** the thumb-adjacent deformable palmar area due to thumb CMC joint motion (abduction/adduction and opposition); **FZ-III-2** the finger-adjacent deformable palmar area due to finger MCP joints (abduction/adduction and MCP bending); **FZ-III-3** the central area with negligible deformation; **FZ-III-4** the deformable palmar area due to axial folding of the palm by CMC IV&V joints. As a result, the palm was far from a rigid area during hand motions, but the majority (FZ-III-1, 2, 4) could deform substantially. Only FZ-III-3 could be regarded as stationary, as shown in Figure 2(e), similar to a human hand.

Following the above discussions, we propose the BCL-26 hand design with 26 independent DOFs from 22 actuators, which matched exactly with the 22 joints in the 22-DOF human hand model in Figure 2(f) [60]. Since the 4 X-actuators (13-16) each had 2 independent actuations

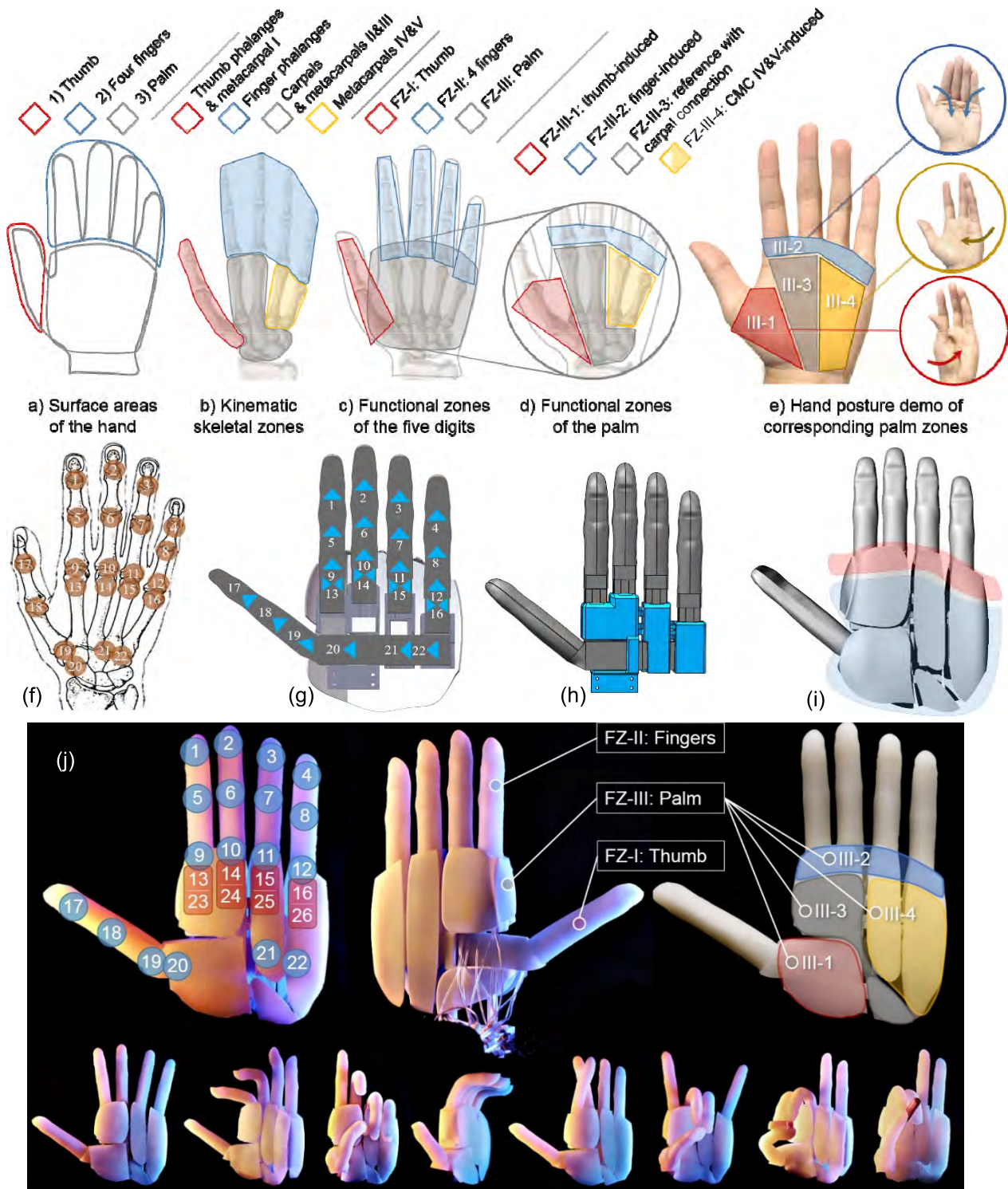


FIGURE 2. (a-b) Conventional approaches to human hand surface partitioning; (c-d) Proposed anatomically-correct partitioning of the human hand, with 3 Functional Zones and 4 sub-zones for the palm; (e) the palm is not a rigid area: only FZ-III-3 stationary, all other areas could deform; (f) commonly adopted 22-DOF human hand model in [60]; (g) DOF and actuator arrangements, with 18 V-chamber actuators (1-12, 17-22) and 4 Xchamber actuators (13-16, doubling as 22-26), totaling 26 independently actuated DOFs; (h) design of whole hand with 5 digits, with soft (grey) material digits mounted on rigid (blue) supporting components; (i) design of palmar area with rigid inner layer (grey) and soft outer layer (red); (j) fabricated prototype of the BCL-26 hand.

realizing 2 independent DOFs (abduction/adduction and axial extension), they represented 8 DOFs: 4 for the abduction/adduction (13-16), and an additional 4 for the axial

extensions (23-26) for each finger, totaling 26 independent DOFs for the BCL-26 hand (Figure 2(g)). The structural component of the hand comprised of 3 parts: a rigid core piece

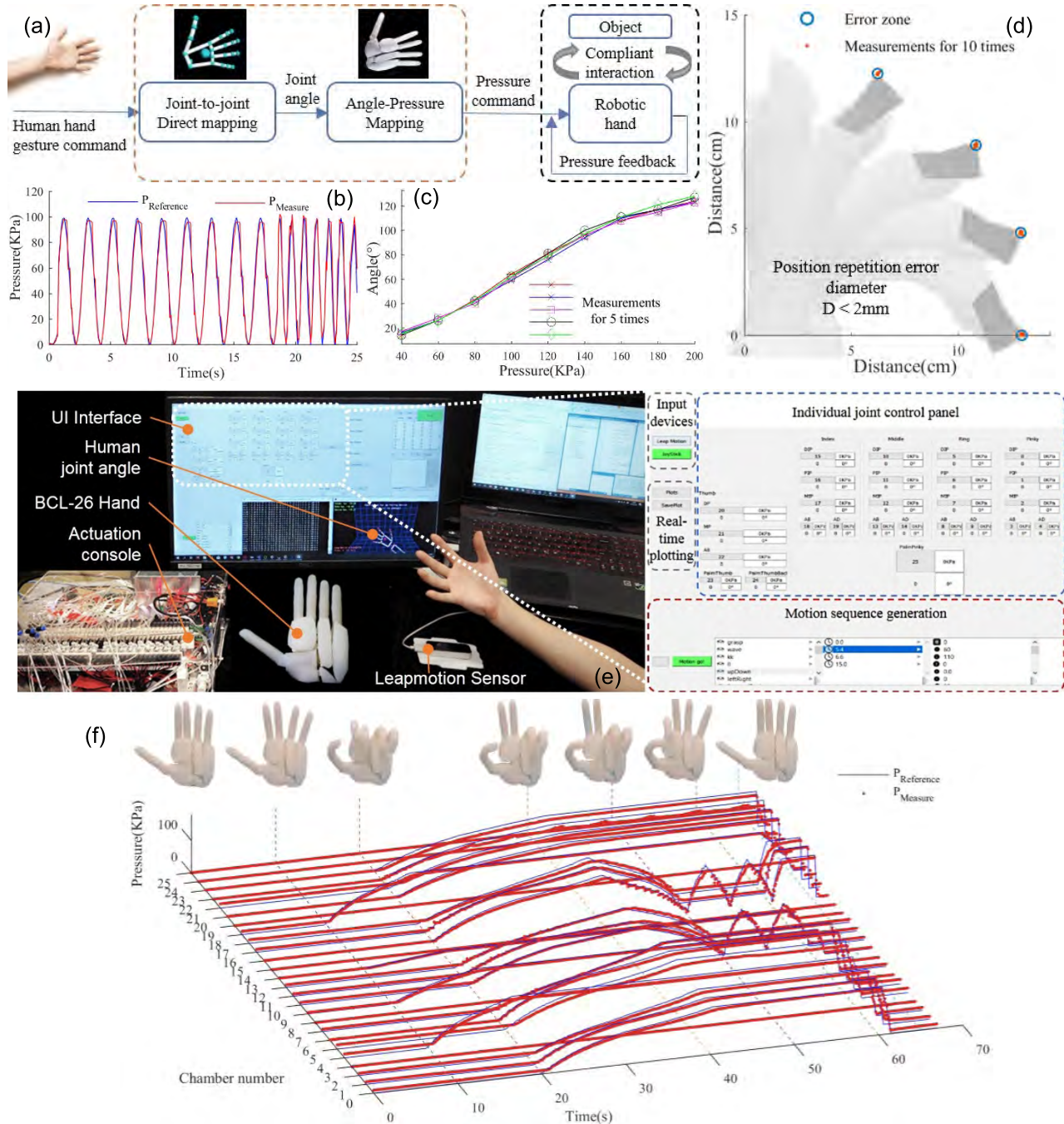


FIGURE 3. Actuation and control. (a) Controller scheme of the proposed cascaded controller with hybrid close-loop pressure control and open-loop angle control; (b) Pressure tracking control could follow 1Hz reference pressure commands with RMSE<10kPa; (c) Angle tracking control could reach 4% RMSE of maximum motion range, sufficient for daily tasks; (d) Position tracking results of one finger, 10-time repetitive results with error $D < 2\text{mm}$; (e) Control hardware and UI interface; (f) Intuitive control with human hand gesture, pressure commands of all 26 chambers following realtime human hand gesture sequence.

corresponding to the carpal bones and the metacarpal 2&3 of the human hand connected the index and middle finger to the base of the hand; while two extension pieces corresponding to the metacarpal 4&5 of the human hand connected the ring and little fingers to the core piece with hinged rotations enabled. The thumb assembly, with the 2-DOF thumb and the 2-DOF thumb-CMC, was also mounted to the core piece. The resulting design assembly was shown in Figure 2(h). A dual-layer

palm design was introduced in BCL-26, with a rigid inner layer connecting to the hand structural components, and an outer soft layer for contact enhancement: the inner layer covered FZ-III-1, FZ-III-3, and FZ-III-4 (grey shaded area of Figure 2(i)), while the outer soft layer covered all 4 zones, leaving the FZ-III-2 only with soft coverage, therefore being able to conform during manipulations (red shaded area of Figure 2(i)).

III. ACTUATION & CONTROL

The large number of DOFs and the nonlinear nature of each actuator brought substantial challenges to the actuation and control of BCL-26. In this work we chose pneumatic drive over hydraulics, for its compressibility, lightweight, and compactness advantages [75]. The actuation and control strategies covered in this article were aimed at enabling the basic operation of the BCL-26 hand, in order to demonstrate its characteristics and novelties.

A. MULTI-CHANNEL HARDWARE PLATFORM

To facilitate the high number of independent chambers incorporated in BCL-26, an actuation console was developed with 32 independent pneumatic actuation channels (Figure 3(e)). Each channel was equipped with a dedicated pneumatic sensor and dual regulated valves. All channels were connected to both positive (compressor) and negative (vacuum) pressure sources. The console was controlled by MCU with a sampling frequency of 1kHz. Further details of the actuation console are included in the Supplementary Materials.

To control the BCL-26 hand coordinately of the total 26 chambers, the following two critical challenges must be addressed: i) control of a single actuator/joint in reaching a desired target; ii) coordinated control and command generation to drive all joints simultaneously.

B. SINGLE JOINT CONTROL

The advanced control of a pneumatic actuator has been studied in [76], [77]. In this work, a conventional cascade control structure [78] was employed (Figure 3(a)), with two cascaded layers: the inner layer with faster sampling rates (at 1kHz) employed air pressure control; while the outer layer with open loop angle control. Our previous works have repeatedly demonstrated that this hybrid control structure could sufficiently drive soft actuators to perform desired tasks ([45], [49], [53], [57]). Extensive experiments had been carried out on the novel soft actuator designs, with highlighted results shown in Figure 3(b, c). For pressure control, the high-frequency inner loop could successfully track a reference pressure command of 1Hz with RMS error $<10\text{kPa}$ (Figure 3(b)); while for angle control, the hybrid cascaded controller could achieve very accurate angle tracking results with 5-time repetitive RMS error of 2 degrees, or 1.9% of maximum motion range, well within the typical range of passive deflection of soft actuators (around 5%), as shown in Figure 3(c).

C. WHOLE HAND CONTROL

Two different approaches were adopted to control the BCL-26 hand towards different applications. i) For real-time grasping tasks or en-bloc gesture control tasks, we developed an intuitive control workflow by direct capturing of human hand gesture and joint angles, motion mapping the obtained information into the robotic hand joints, and finally controlling the real-time joint angle of the BCL-26 hand.

The workflow was based on our previous work [79], fundamentally redesigned to extract human joint angles and matched with the 26-DOF new hand. ii) For fine in-hand manipulation, or tasks involving individual joint angle assignments, a fully-computerized controller was developed, with a user interface where the user could get access to each individual joint angle, or set time-series of angle reference trajectories (Figure 3(e)).

Implementation of the whole hand control comprised of three key components, as shown in Figure 3(a). **Trajectory generation** was utilized with a commercial leap-motion sensor [80] to directly obtain human hands trajectory. In case of poor measurement quality (due to occlusion or noise), direct motion sequences could be generated by interpolating key frames. **Angle mapping** was then carried out for the open outer loop, from the angle commands to corresponding pressure commands, using experimentally extracted mapping functions. **Pressure feedback control** was finally carried out for each chamber, with individual pressure regulated by controlling two pulse-wide modulated (PWM) solenoid valves for inflating and deflating, respectively. By adjusting the PWM duty cycles of the valves, we could regulate the flow rate and eventually the chamber pressure.

Results of the whole hand controller were shown in Figure 3(d, f). For fingertip positioning, the repetition error of 10-time repetition was $<2\text{mm}$, sufficient for most daily tasks (Figure 9(d)). The intuitive human-hand control results were shown in Figure 9(e), with the pressure commands for each of the 26 chambers spread in a 3-D plot, showing the timed sequences of commands, when the human hand followed a series of gesture sequences as illustrated by the BCL-26 hands listed on top. Following this approach, the BCL-26 hand could follow the human commands timely, performing free-space gestures, as well as grasping tasks. The dynamic process of the intuitive controller performance in object grasping was included in the Supplementary Video.

The payload capability of the BCL-26 hand was validated by an object-pull-out test as introduced in [55]. The maximum holding force to a standard spherical object was 21.9N on the vertical direction, with a maximum diameter of xxx mm. Further results on control and evaluations were included in the Supplementary Materials.

IV. PERFORMANCE OF BCL-26 HAND

The performance results are presented in the following three clusters: first, validate that the BCL-26 could complete (i) the grasping taxonomy, (ii) Kapandji thumb dexterity test, and (iii) in-hand manipulation taxonomy.

A. GRASPING TAXONOMY

In this experiment, the BCL-26 prototype was used to grasp a series of benchmark objects as listed out in the GRASP taxonomy with 33 grasping types [67]. The hand was controlled with the dedicated actuation console, with individual joint angles and trajectories set via the user interface of the controller. As shown in the results presented in Figure 4(a),

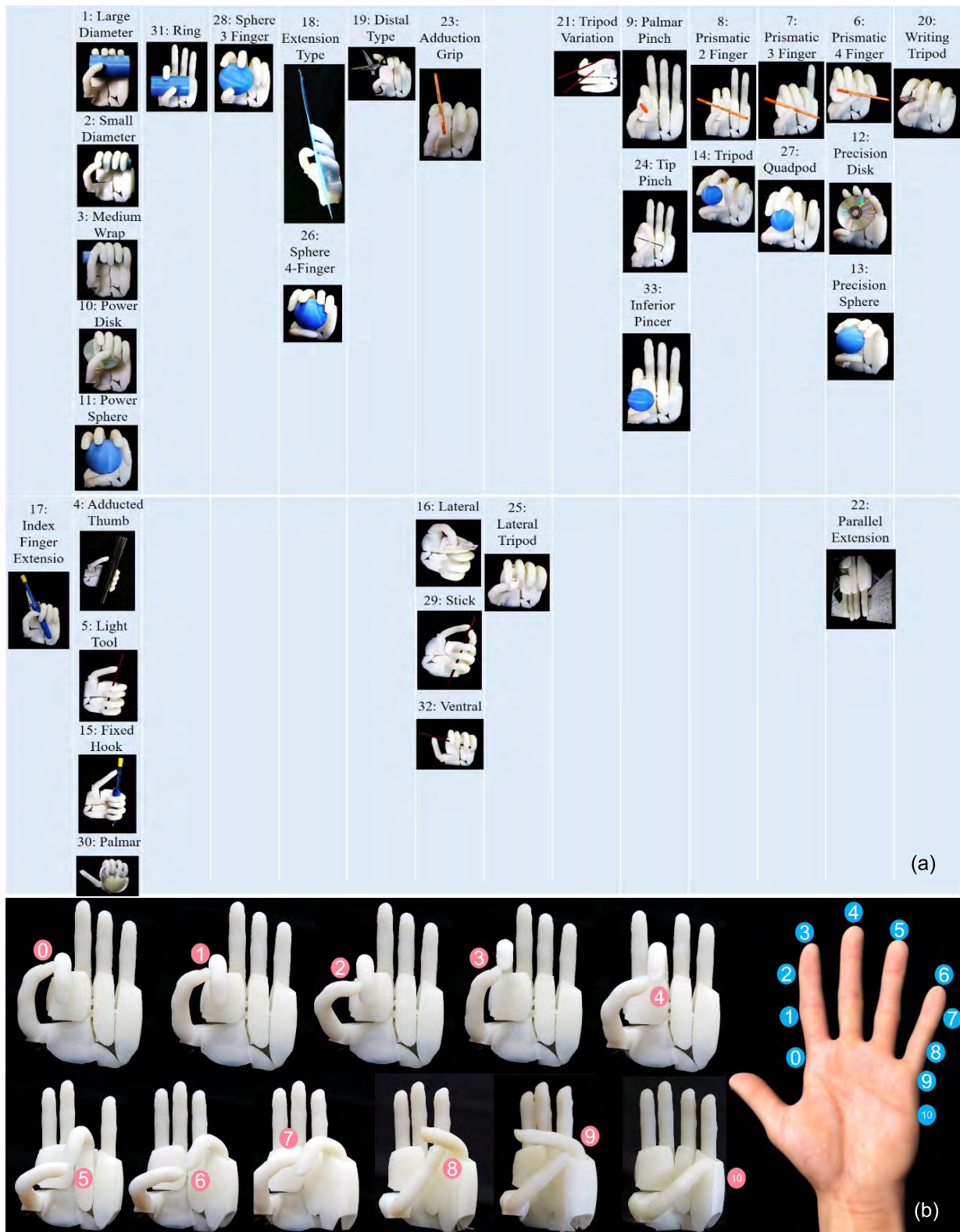


FIGURE 4. The proposed BCL-26 soft robotic hand successfully completed dexterity benchmarks: (a) the GRASP taxonomy with all 33 postures, and (b) the 11-score Kapandji test on thumb dexterity.

the BCL-26 hand could successfully complete all 33 grasping types as listed in the GRASP taxonomy. With the excellent dexterity enabled by the 22 anthropomorphic joints with

individual actuation, most of the grasping postures were achieved with little complications. The most challenging posture was the distal type (#19): although the hand design

was generic and was not optimized for the particular task, it could open and close the scissor within a certain range by coordinately moving its fingers. The dynamic procedure for the distal type grasp (#19) is included in the supplementary video.

B. THUMB DEXTERITY

In this experiment, the BCL-26 hand was used to tackle the Kapandji thumb test with 11 scores [70]. With the anthropomorphic design of BCL-26, the target points on the robotic hand could be clearly identified, closely matching the corresponding target points on a human hand, as shown in Figure 4(b). The thumb of the prototype BCL-26 was controlled across its maximum range of opposition from the dorsal side to the palmar side, with the corresponding fingers bending inward, successfully completing the 11-score Kapandji test.

C. IN-HAND MANIPULATION

In evaluating in-hand manipulation capabilities of BCL-26, we adopted the same manipulation taxonomy benchmark [68]. The object was also adapted from the benchmark: a can of drink. With the object in grasp as the main target of concern, the 6 variations of in-hand manipulation motions were considered: translations and rotations along the x-, y-, and z-axes. During the experiment, the hand was fix-mounted on a rigid base, and during the manipulation at least one contact point between the hand and the object had no relative motion, such that no slippage occurred. All 6 taxonomies of in-hand manipulations were successfully achieved, with results presented in Figure 5(a-f). For the translational motions, the Z-axis (up/down, 13mm) and Y-axis (left/right, 15mm) were comparable, mostly due to the object size was comparable to the hand opening size, leaving limited range of in-hand manipulation; while the X-axis (front/back, 39mm) was nearly 300% that of the other two axes. However, in order to achieve the large-range in-hand manipulation along X-axis, the tips of the thumb and the opposing fingers must move along the same parallel trajectory along the X-axis, in order to translate the object without slipping. To achieve this, independent joint angle control was a necessity, as well as large range joint-like bending, both credited to the proposed V-chamber soft actuators. For the rotational motions, the Z-axis (87 degrees) and X-axis (79 degrees) shown similar results, while Y-axis rotation was noticeably smaller (46 degrees), also due to the limited range of common workspace resulting from large object size.

Two new patterns of in-hand manipulation are also shown, further to the 6 in-hand manipulation taxonomies: **i) juggling a pen** with the index and middle fingers between the MCP and PIP joints (Figure 5(g)), with abduction/adduction and MCP joints independently controlled, this pattern of pen juggling could reach 95 degrees around the Z-axis, a nearly 10% increase from the benchmark results in Figure 5(d); **ii) swaying a card** held between index and middle finger (or any adjacent two fingers), demonstrating the abduction/

adduction capability of the hand, achieving 31 degrees around the X-axis, as shown in Figure 5(h). The two new patterns demonstrated new ways of manipulating an object using in-hand manipulation, closely resembling human hand behaviors.

V. FURTHER INVESTIGATIONS ON THE BCL-26 HAND PLATFORM

With the proposed BCL-26 hand, it is possible for further investigations on hand dexterity, control, and even hand design iterations. Here three performance results were presented on very distinctive aspects: win-hand writing with BCL-26 to showcase the excellent dexterity of the hand itself; independency of DIP/PIP/MCP joints to investigate the human hand nature conversely; and metacarpal extensions on new design-oriented possibilities.

A. IN-HAND WRITING FOR ROBOTIC HANDS

While robotic hand writing was traditionally achieved by the dexterous manipulator generating the writing motion with the fixed hand holding a pen [72], [73], this was not the common practice for humans. For human writing, the wrist is anchored on the desk, while the majority of the writing motion was generated from the fingers, hence the concept of **in-hand writing**. Using the BCL-26 with excellent dexterity, we could demonstrate the first soft robotic in-hand writing, achieved with the robotic hand fixed on a mounting base and only using in-hand manipulation of the pen to draw series of strokes. The enabling factor to this feature was the passive deflection of the soft fingers. As shown in Figure 6(a), finger abduction could only move the finger laterally for a very limited range (middle figure), compared with the natural resting position (left figure), while using the thumb to passively deflect the index finger could achieve substantially larger range of motion (right figure). Benefiting from passive deflection of the BCL-26 hand, in this experiment, the prototype hand held a pen using the thumb against the index and middle fingers, as shown in Figure 6(b), forming a tripod precision grasp (GRASP taxonomy #20). For a horizontal stroke, the thumb was the leading digit, while the two fingers followed passively; for a vertical stroke (19mm), the index finger generated the motion, while the thumb and middle finger followed passively. As shown in the results, when drawing a horizontal stroke of 26mm, the middle finger was already deflected from its axial center, where no actuator in the middle finger could generate such motion. Passive deflection clearly extended the range of the writing motion.

B. INDEPENDENCY OF DIP/PIP/MCP JOINTS

The DIP and PIP joints are coupled (independent from MCP) for the human hand for all fingers, which was also adopted by the vast majority of anthropomorphic robotic hands and even multi-jointed industrial grippers. However, the DIP/PIP/MCP joints are independent for the BCL-26, enabling the investigation on the implications of fully-independent finger joints. The motion characteristics of the fully-independent joints

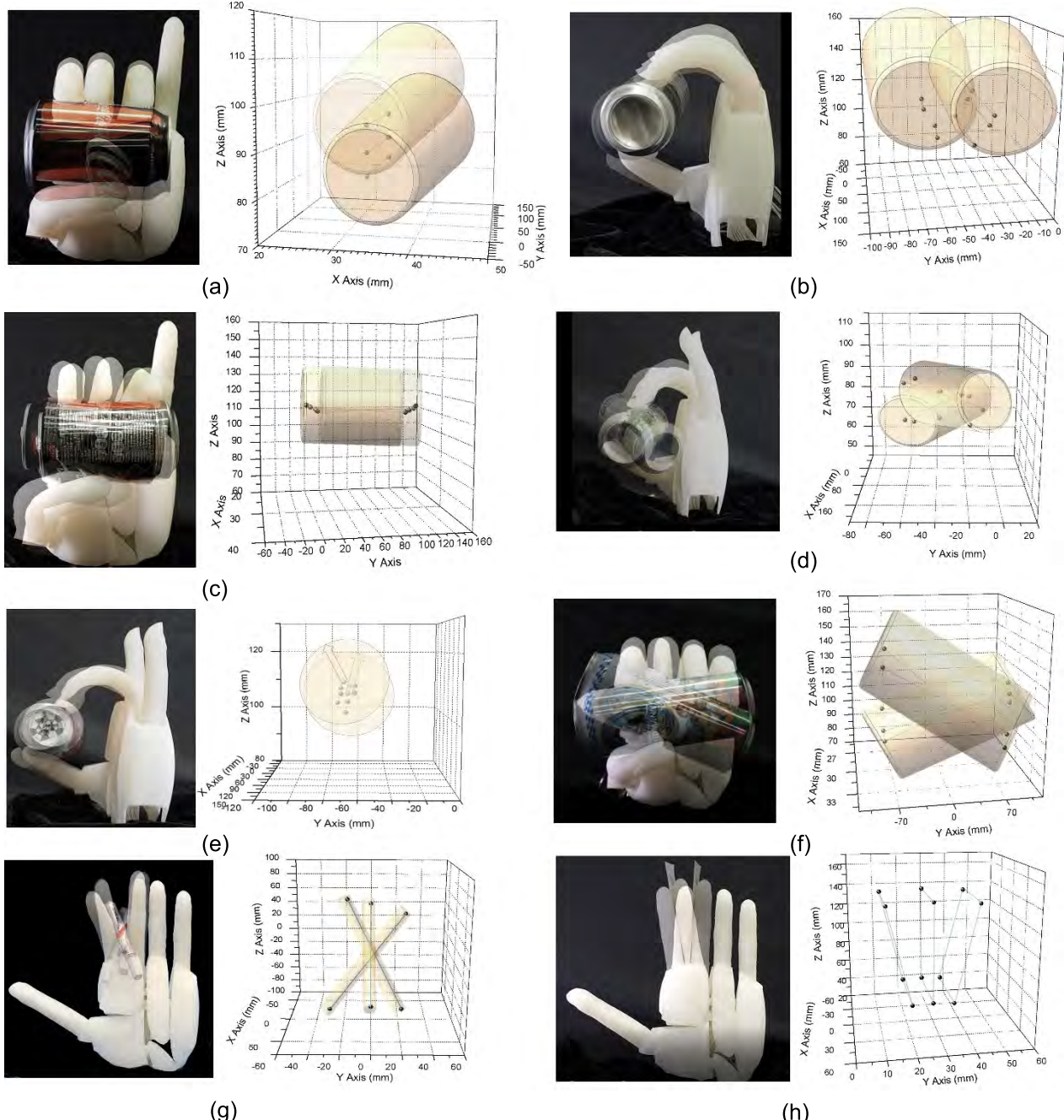


FIGURE 5. In-hand manipulation performance of BCL-26, overlaid snapshots and max motion range results. (a) Z-translation; (b) X-translation; (c) Y-translation; (d) Z-rotation; (e) Y-rotation; (f) X-rotation; (g) new pattern 1: Pen juggling; (h) new pattern 2: Card swaying.

of BCL-26 was demonstrated in Figure 6(c), where each finger joint could be separately actuated, distinctive from the human hand. Enabled by this feature, this study was divided into two aspect: **tip reachability** and **tip orientation**. i) for fingertip reachable space, as shown in Figure 6(d), a finger of BCL-26 was placed at (0, 0) in the coordinate frame and stretched long the positive horizontal axis pointing to the right. The maximum reachable space of the fingertip was plotted as the finger was actuated, either fully independently,

or with coupled PIP/DIP joints. The resulting differences between the two plots were less than 5% in area, slightly larger for the fully independent joints. However, this minor advantage in reachable area could be easily compromised by the passive deflection of soft robots. ii) for fingertip orientation, the improvements were substantial with independent joints. Without independent DIP/PIP, the finger was able to reach a target location in the reachable space only with one possible solution, i.e. with one orientation; on the contrary,

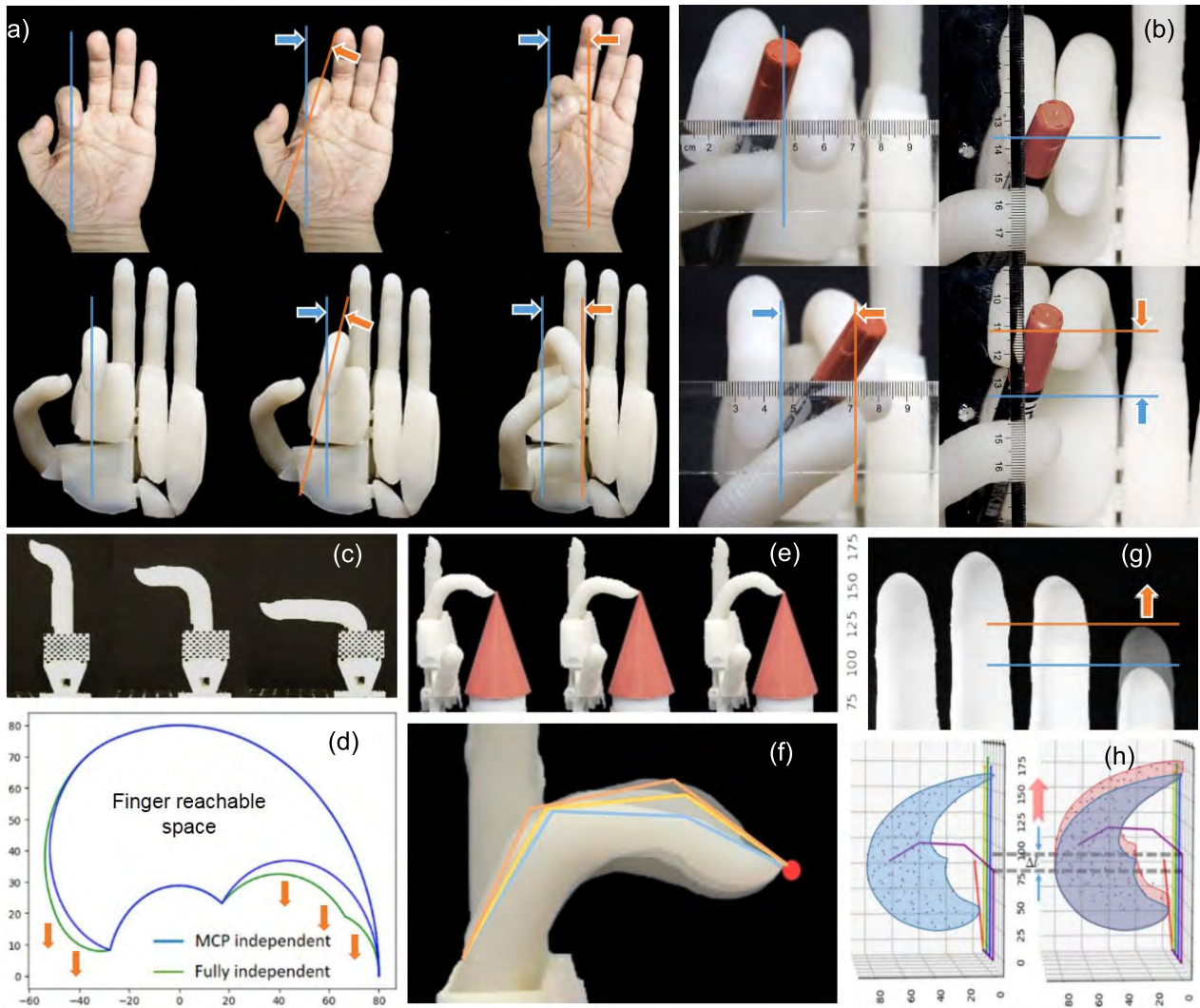


FIGURE 6. Further investigations enabled by the BCL-26 platform. (a) BCL-26 resembled human finger passive deflection; (b) in-hand writing with vertical (19mm) and horizontal (26mm) strokes; (c) reachable space comparison for independent DIP/PIP/MCP joints; (d) reachable workspace with fully independent joints; (e-f) multiple orientations of reaching a same target location; (g) metacarpal extension; (h) simulation results on reachable space with metacarpal extension.

with independent DIP/PIP, the three revolute joints formed a manipulator with redundancy, therefore could reach a point in its workspace from a range of different orientations. The demonstration of this result was shown in Figure 6(e-f), with the base of the finger mounted at a fixed location, the fingertip could reach the same target location (tip of the cone) from different orientations.

Following the above discussions, if reachability was the primary concern (presumably true for the human hand in most grasping and manipulation tasks), then independent control of DIP/PIP joints was not critically required, or the less than 5% increase in workspace could easily be outweighed by saving one individual actuation, which could significantly reduce energy consumption and system complexity. This study could offer some insights on why our biological hand took a coupled, rather than independent approach with the DIP/PIP joints.

C. UNIQUE METACARPAL EXTENSION OF BCL-26

The X-actuators used in the MCP joints (13-16) could each generate 2 DOFs. The elongation motion of each X-actuator resulted in the extension of the metacarpal link for each finger. The resulting 4 new DOFs of metacarpal extension were not seen in any previous biological or robotic hands. Here we explore the implication and possibilities of having metacarpal extension in a robotic hand. A simulation of maximum reachable workspace was conducted, with results shown in Figure 6(g), where a 10% metacarpal extension (to overall finger length) could result in over 15% increase in reachable workspace, more prominent than DIP joint independency. Experiments were then conducted on the prototype BCL-26, on the reachability of the finger with metacarpal extension enabled. For each finger, there were now 5 DOFs in total. Extending the metacarpal link was effectively shifting the original reachable space of the finger up and down along

the vertical z-axis, as shown in Figure 6(h). The dynamic process of extending the metacarpal link was included in the Supplementary video.

VI. CONCLUSIONS AND FUTURE WORK

It has been demonstrated that introducing passive compliance into robotic hands could impose drastic changes to certain dexterity measures. The most-affected grasping taxonomy, in comparison with the least-affected in-hand manipulation, could substantially reduce the mechanistic complexity requirement. In addition, it was also demonstrated that passive compliance could substantially increase the range of motion for a finger, contributing to in-hand writing. It was worth noting, that low-DOF, high compliance soft robots could achieve excellent functional dexterity. In a more general perspective, the passive compliance of links and joints were enabled by the compliance of the materials and components. While rigid robots must rely on special components (flexible cable, elastic link, etc.) to achieve passive compliance, compliance is naturally embedded in soft robotic components as an inherent feature without requiring special design consideration.

We have discussed a novel 26-DOF soft robotic hand design, the most dexterous soft robotic hand to-date, with dexterity performance validations, prototype systems and validation experiments. Speed was not considered, as it was the well-known limitations of soft robots. A hybrid approach with soft actuators driving rigid structural components had been proven with desirable benefits in this regard, it could be explored in future investigations.

ACKNOWLEDGMENT

(Jianshu Zhou and Xiaojiao Chen contributed equally to this work.)

REFERENCES

- [1] M. W. Marzke, “Tool making, hand morphology and fossil hominins,” *Philos. Trans. Roy. Soc. B, Biol. Sci.*, vol. 368, Nov. 2013, Art. no. 20120414.
- [2] T. L. Kivell, “Evidence in hand: Recent discoveries and the early evolution of human manual manipulation,” *Philos. Trans. Roy. Soc. B, Biol. Sci.*, vol. 370, Nov. 2015, Art. no. 20150105.
- [3] G. J. Monkman, S. Hesse, and R. Steinmann, *Robot Grippers*. Hoboken, NJ, USA: Wiley, 2007.
- [4] A. H. Al-Timemy, G. Bugmann, J. Escudero, and N. Outram, “Classification of finger movements for the dexterous hand prosthesis control with surface electromyography,” *IEEE J. Biomed. Health Inform.*, vol. 17, no. 3, pp. 608–618, May 2013.
- [5] B. Massa, S. Roccella, M. C. Carrozza, and P. Dario, “Design and development of an underactuated prosthetic hand,” in *Proc. IEEE Int. Conf. Robot. Automat.*, May 2002, pp. 3374–3379.
- [6] J. T. Belter and A. M. Dollar, “Performance characteristics of anthropomorphic prosthetic hands,” in *Proc. IEEE Int. Conf. Rehabil. Robot.*, Jul. 2011, pp. 1–7.
- [7] L. Zollo, S. Roccella, E. Guglielmelli, M. C. Carrozza, and P. Dario, “Biomechatronic design and control of an anthropomorphic artificial hand for prosthetic and robotic applications,” *IEEE/ASME Trans. Mechatronics*, vol. 12, no. 4, pp. 418–429, Aug. 2007.
- [8] W. Chen, C. Xiong, and S. Yue, “Mechanical implementation of kinematic synergy for continual grasping generation of anthropomorphic hand,” *IEEE/ASME Trans. Mechatronics*, vol. 20, no. 3, pp. 1249–1263, Jun. 2015.
- [9] A. M. Dollar and R. D. Howe, “The highly adaptive SDM hand: Design and performance evaluation,” *Int. J. Robot. Res.*, vol. 29, no. 5, pp. 585–597, 2010.
- [10] H. Kawasaki, T. Komatsu, and K. Uchiyama, “Dexterous anthropomorphic robot hand with distributed tactile sensor: Gifu hand II,” *IEEE/ASME Trans. Mechatronics*, vol. 7, no. 3, pp. 296–303, Sep. 2002.
- [11] M. Grebenstein, M. Chalon, W. Friedl, S. Haddadin, T. Wimböck, G. Hirzinger, and R. Siegwart, “The hand of the DLR hand arm system: Designed for interaction,” *Int. J. Robot. Res.*, vol. 31, no. 13, pp. 1531–1555, Nov. 2012.
- [12] M. Reichel, “Transformation of shadow dexterous hand and shadow finger test unit from prototype to product for intelligent manipulation and grasping,” in *Proc. Intell. Manipulation Grasping, Inter. Conf.*, Jul. 2010, p. 70.
- [13] L. U. Odhner, L. P. Jenoft, M. R. Claffee, N. Corson, Y. Tenzer, R. R. Ma, M. Buehler, R. Kohout, R. D. Howe, and A. M. Dollar, “A compliant, underactuated hand for robust manipulation,” *Int. J. Robot. Res.*, vol. 33, no. 5, pp. 736–752, 2014.
- [14] C. S. Lovchik and M. A. Diftler, “The Robonaut hand: A dexterous robot hand for space,” in *Proc. IEEE Int. Conf. Robot. Automat.*, May 1999, pp. 907–912.
- [15] H. Liu, K. Wu, P. Meusel, N. Seitz, G. Hirzinger, M. H. Jin, Y. W. Liu, S. W. Fan, T. Lan, and Z. P. Chen, “Multisensory five-finger dexterous hand: The DLR/HIT Hand II,” in *Proc. IEEE/RSJ Int. Conf. Intell. Robots Syst.*, Sep. 2008, pp. 3692–3697.
- [16] A. Bicchi, “Hands for dexterous manipulation and robust grasping: A difficult road toward simplicity,” *IEEE Trans. Robot. Autom.*, vol. 16, no. 6, pp. 652–662, Dec. 2000.
- [17] A. Bicchi and V. Kumar, “Robotic grasping and contact: A review,” in *Proc. ICRA*, Apr. 2000, pp. 348–353.
- [18] D. Prattichizzo and J. C. Trinkle, *Grasping In Springer Handbook of Robotics*. Springer, Berlin, Heidelberg, Germany, 2008.
- [19] M. V. Weghe, M. Rogers, M. Weissert, and Y. Matsuoka, “The ACT Hand: Design of the skeletal structure,” in *Proc. IEEE Int. Conf. Robot. Automat.*, May 2004, pp. 3375–3379.
- [20] A. D. Deshpande, Z. Xu, M. J. V. Weghe, B. H. Brown, J. Ko, L. Y. Chang, D. D. Wilkinson, S. M. Bidic, and Y. Matsuoka, “Mechanisms of the anatomically correct testbed hand,” *IEEE/ASME Trans. Mechatronics*, vol. 18, no. 1, pp. 238–250, Feb. 2013.
- [21] Z. Xu and E. Todorov, “Design of a highly biomimetic anthropomorphic robotic hand towards artificial limb regeneration,” in *Proc. IEEE Int. Conf. Robot. Automat. (ICRA)*, May 2016, pp. 3485–3492.
- [22] J. A. E. Hughes, P. Maiolino, and F. Iida, “An anthropomorphic soft skeleton hand exploiting conditional models for piano playing,” *Sci. Robot.*, vol. 3, no. 25, 2018, Art. no. eaau3098.
- [23] R. R. Ma, L. U. Odhner, and A. M. Dollar, “A modular, open-source 3D printed underactuated hand,” in *Proc. IEEE Int. Conf. Robot. Automat.*, May 2013, pp. 2737–2743.
- [24] T. Iberall, “The nature of human prehension: Three dextrous hands in one,” in *Proc. IEEE Int. Conf. Robot. Automat.*, Apr. 1987, pp. 396–401.
- [25] A. M. Dollar and R. D. Howe, “Joint coupling design of underactuated hands for unstructured environments,” *Int. J. Robot. Res.*, vol. 30, no. 9, pp. 1157–1169, Aug. 2011.
- [26] M. Santello, M. Flanders, and J. F. Soechting, “Postural hand synergies for tool use,” *J. Neurosci.*, vol. 18, no. 23, pp. 10105–10115, Dec. 1998.
- [27] A. Bicchi, M. Gabiccini, and M. Santello, “Modelling natural and artificial hands with synergies,” *Philos. Trans. Roy. Soc. B, Biol. Sci.*, vol. 366, pp. 3153–3161, Nov. 2011.
- [28] M. T. Ciocarlie and P. K. Allen, “Hand posture subspaces for dexterous robotic grasping,” *Int. J. Robot. Res.*, vol. 28, no. 7, pp. 851–867, Jul. 2009.
- [29] C. Goldfeder, M. Ciocarlie, H. Dang, and P. K. Allen, “The Columbia grasp database,” in *Proc. IEEE Int. Conf. Robot. Automat.*, May 2009, pp. 1710–1716.
- [30] M. H. Schieber and M. Santello, “Hand function: Peripheral and central constraints on performance,” *J. Appl. Physiol.*, vol. 96, no. 6, pp. 2293–2300, Jun. 2004.
- [31] S. Cobos, M. Ferre, and R. Aracil, “Simplified human hand models based on grasping analysis,” in *Proc. IEEE/RSJ Int. Conf. Intell. Robots Syst.*, Oct. 2010, pp. 610–615.
- [32] G. C. Matrone, C. Cipriani, E. L. Secco, G. Magenes, and M. C. Carrozza, “Principal components analysis based control of a multi-dof underactuated prosthetic hand,” *J. Neuroeng. Rehabil.*, vol. 7, no. 1, p. 16, 2010.
- [33] C. Majidi, “Soft robotics: A perspective—Current trends and prospects for the future,” *Soft Robot.*, vol. 1, no. 1, pp. 5–11, 2014.

- [34] J. Zhou, S. Chen, and Z. Wang, "A soft-robotic gripper with enhanced object adaptation and grasping reliability," *IEEE Robot. Autom. Lett.*, vol. 2, no. 4, pp. 2287–2293, Oct. 2017.
- [35] R. R. Deimel and O. Brock, "A novel type of compliant and underactuated robotic hand for dexterous grasping," *Int. J. Robot. Res.*, vol. 35, pp. 161–185, Jan. 2016.
- [36] K.-J. Cho, J. Rosmarin, and H. Asada, "SBC hand: A lightweight robotic hand with an SMA actuator array implementing C-segmentation," in *Proc. IEEE Int. Conf. Robot. Automat.*, Apr. 2007, pp. 921–926.
- [37] Y. Wei, Y. Chen, T. Ren, Q. Chen, C. Yan, Y. Yang, and Y. Li, "A novel, variable stiffness robotic gripper based on integrated soft actuating and particle jamming," *Soft Robot.*, vol. 3, no. 3, pp. 134–143, Sep. 2016.
- [38] D.-H. Lee, J.-H. Park, S.-W. Park, M.-H. Baeg, and J.-H. Bae, "KITECH-hand: A highly dexterous and modularized robotic hand," *IEEE/ASME Trans. Mechatronics*, vol. 22, no. 2, pp. 876–887, Apr. 2017.
- [39] H. Zhao, K. O'Brien, S. Li, and R. F. Shepherd, "Optoelectronically innervated soft prosthetic hand via stretchable optical waveguides," *Sci. Robot.*, vol. 1, no. 1, Dec. 2016, Art. no. eaai7529.
- [40] K. Hosoda, Y. Tada, and M. Asada, "Anthropomorphic robotic soft fingertip with randomly distributed receptors," *Robot. Auton. Syst.*, vol. 54, no. 2, pp. 104–109, 2006.
- [41] H. Yousef, M. Boukallel, and K. Althoefer, "Tactile sensing for dexterous in-hand manipulation in robotics-A review," *Sens. Actuators A, Phys.*, vol. 167, no. 2, pp. 171–187, 2011.
- [42] J. T. Belter, J. L. Segil, A. M. Dollar, and R. F. Weir, "Mechanical design and performance specifications of anthropomorphic prosthetic hands: A review," *J. Rehabil. Res. Develop.*, vol. 50, no. 5, pp. 599–618, 2013.
- [43] A. D. Marchese, R. K. Katzschmann, and D. Rus, "A recipe for soft fluidic elastomer robots," *Soft Robot.*, vol. 2, no. 2, pp. 7–25, Mar. 2015.
- [44] C. Laschi, M. Cianchetti, B. Mazzolai, L. Margheri, M. Follador, and P. Dario, "Soft robot arm inspired by the octopus," *Adv. Robot.*, vol. 26, no. 7, pp. 709–727, Jan. 2012.
- [45] P. Polygerinos, Z. Wang, K. C. Galloway, R. J. Wood, and C. J. Walsh, "Soft robotic glove for combined assistance and at-home rehabilitation," *Robot. Auton. Syst.*, vol. 73, pp. 135–143, Nov. 2015.
- [46] F. Ilievski, A. D. Mazzeo, R. F. Shepherd, X. Chen, and G. M. Whitesides, "Soft robotics for chemists," *Angew. Chem. Int. Ed.*, vol. 123, no. 8, pp. 1890–1895, Feb. 2011.
- [47] J. T. Overvelde, Y. Mengüç, P. Polygerinos, Y. Wang, Z. Wang, C. J. Walsh, R. J. Wood, and K. Bertoldi, "Mechanical and electrical numerical analysis of soft liquid-embedded deformation sensors analysis," *Extreme Mech. Lett.*, vol. 1, pp. 42–46, Dec. 2014.
- [48] Y. She, C. Li, J. Cleary, and H. J. Su, "Design and fabrication of a soft robotic hand with embedded actuators and sensors," *J. Mech. Robot.*, vol. 7, no. 7, 2015, Art. no. 021007.
- [49] X. Chen, J. Yi, J. Li, J. Zhou, and Z. Wang, "Soft-actuator-based robotic joint for safe and forceful interaction with controllable impact response," *IEEE Robot. Autom. Lett.*, vol. 3, no. 4, pp. 3505–3512, Oct. 2018.
- [50] P. Polygerinos, Z. Wang, J. T. Overvelde, K. C. Galloway, R. J. Wood, K. Bertoldi, and C. J. Walsh, "Modeling of soft fiber-reinforced bending actuators," *IEEE Trans. Robot.*, vol. 31, no. 3, pp. 778–789, Jun. 2015.
- [51] Z. Wang, P. Polygerinos, J. T. Overvelde, K. C. Galloway, K. Bertoldi, and C. J. Walsh, "Interaction forces of soft fiber reinforced bending actuators," *IEEE/ASME Trans. Mechatronics*, vol. 22, no. 2, pp. 717–727, Apr. 2017.
- [52] Y. Yang, Y. Chen, Y. Li, Z. Wang, and Y. Li, "Novel Variable-stiffness robotic fingers with built-in position feedback," *Soft Robot.*, vol. 4, no. 4, pp. 338–352, Dec. 2017.
- [53] J. Yi, X. Chen, C. Song, J. Zhou, Y. Liu, S. Liu, and Z. Wang, "Customizable three-dimensional-printed origami soft robotic joint with effective behavior shaping for safe interactions," *IEEE Trans. Robot.*, vol. 35, no. 1, pp. 114–123, Oct. 2018.
- [54] A. Gupta, C. Eppner, S. Levine, and P. Abbeel, "Learning dexterous manipulation for a soft robotic hand from human demonstrations," in *Proc. IEEE/RSJ Int. Conf. Intell. Robots Syst. (IROS)*, Oct. 2016, pp. 3786–3793.
- [55] J. Zhou, J. Yi, X. Chen, Z. Liu, and Z. Wang, "BCL-13: A 13-DOF Soft robotic hand for dexterous grasping and in-hand manipulation," *IEEE Robot. Autom. Lett.*, vol. 3, no. 4, pp. 3379–3386, Oct. 2018.
- [56] M. Manti, T. Hassan, G. Passetti, N. D'Elia, C. Laschi, and M. Cianchetti, "A bioinspired soft robotic gripper for adaptable and effective grasping," *Soft Robot.*, vol. 2, no. 3, pp. 107–116, Sep. 2015.
- [57] J. Yi, X. Chen, C. Song, and Z. Wang, "Fiber-reinforced origamic robotic actuator," *Soft Robot.*, vol. 5, no. 1, pp. 81–92, Feb. 2018.
- [58] K. C. Galloway, K. P. Becker, B. Phillips, J. Kirby, S. Licht, D. Tchernov, R. J. Wood, and D. F. Gruber, "Soft robotic grippers for biological sampling on deep reefs," *Soft Robot.*, vol. 3, no. 1, pp. 23–33, Mar. 2016.
- [59] M. Pozzi, G. Salvietti, J. Bimbo, M. Malvezzi, and D. Prattichizzo, "The closure signature: A functional approach to model underactuated compliant robotic hands," *IEEE Robot. Autom. Lett.*, vol. 3, no. 3, pp. 2206–2213, Jul. 2018.
- [60] J. R. Napier and R. H. Tuttle, *Hands*. Princeton, NJ, USA: Princeton Univ. Press, 1993.
- [61] Z. Li, J. F. Canny, and S. S. Sastry, "On motion planning for dexterous manipulation. I. The problem formulation," in *Proc. Int. Conf. Robot. Automat.*, May 1987, pp. 775–780.
- [62] A. M. Okamura, N. Smaby, and M. R. Cutkosky, "An overview of dexterous manipulation," in *Proc. IEEE Int. Conf. Robot. Autom. (ICRA)*, Apr. 2000, pp. 255–262.
- [63] C. A. Klein and B. E. Blaho, "Dexterity measures for the design and control of kinematically redundant manipulators," *Int. J. Robot. Res.*, vol. 6, no. 2, pp. 72–83, 1987.
- [64] R. R. Ma and A. M. Dollar, "On dexterity and dexterous manipulation," in *Proc. 15th Int. Conf. Adv. Robot. (ICAR)*, Jun. 2011, pp. 1–7.
- [65] J. R. Napier, "The prehensile movements of the human hand," *J. Bone Joint Surg. Brit.*, vol. 38, pp. 902–913, Nov. 1956.
- [66] M. R. Cutkosky, "On grasp choice, grasp models, and the design of hands for manufacturing tasks," *IEEE Trans. Robot. Autom.*, vol. 5, no. 3, pp. 269–279, Jun. 1989.
- [67] T. Feix, J. Romero, H.-B. Schmidmayer, A. M. Dollar, and D. Kragic, "The GRASP taxonomy of human grasp types," *IEEE Trans. Human-Mach. Syst.*, vol. 46, no. 1, pp. 66–77, Feb. 2016.
- [68] I. M. Bullock, R. R. Ma, and A. M. Dollar, "A hand-centric classification of human and robot dexterous manipulation," *IEEE Trans. Haptics*, vol. 6, no. 2, pp. 129–144, Apr. 2013.
- [69] J. C. Colditz, "Anatomic considerations for splinting the thumb," *Rehabil. Hand. Surg. Therapy.*, vol. 30, pp. 1–17, Feb. 1995.
- [70] A. I. Kapandji, "Clinical evaluation of the thumb's opposition," *J. Hand Therapy*, vol. 5, pp. 102–106, Apr. 1992.
- [71] I. Gaiser, S. Schulz, A. Kargov, H. Klosek, A. Bierbaum, C. Pylatiuk, R. Oberle, T. Werner, T. Asfour, G. Bretthauer, and R. Dillmann, "A new anthropomorphic robotic hand," in *Proc. 8th IEEE-RAS Int. Conf. Humanoid Robots*, Dec. 2008, pp. 418–422.
- [72] V. Potkonjak, M. Popovic, M. Lazarevic, and J. Sinanovic, "Redundancy problem in writing: From human to anthropomorphic robot arm," *IEEE Trans. Syst. Man. Cybern. B, Cybern.*, vol. 28, no. 6, pp. 790–805, Dec. 2008.
- [73] P. Liang, C. Yang, Z. Li, and R. Li, "Writing skills transfer from human to robot using stiffness extracted from sEMG," in *Proc. IEEE Int. Conf. Cyber Technol. Automat., Control, Intell. Syst. (CYBER)*, Jun. 2015, pp. 19–24.
- [74] D. Rus and M. T. Tolley, "Design, fabrication and control of soft robots," *Nature*, vol. 521, p. 467, May 2015.
- [75] D. Saravanan Kumar, B. Mohan, and T. Muthuramalingam, "A review on recent research trends in servo pneumatic positioning systems," *Precis. Eng.*, vol. 49, pp. 481–492, Jul. 2017.
- [76] E. Richer and Y. Hurmuzlu, "A high performance pneumatic force actuator system: Part I—Nonlinear mathematical model," *J. Dyn. Syst., Meas., Control*, vol. 122, no. 3, pp. 416–425, Sep. 2000.
- [77] E. Richer and Y. Hurmuzlu, "A high performance pneumatic force actuator system: Part II—Nonlinear controller design," *J. Dyn. Syst., Meas., Control*, vol. 122, no. 3, pp. 426–434, Sep. 2000.
- [78] H. K. Lee, G. S. Choi, and G. H. Choi, "A study on tracking position control of pneumatic actuators," *Mechatronics*, vol. 12, no. 6, pp. 813–831, Jul. 2002.
- [79] J. Zhou, X. Chen, U. Chang, J. Pan, W. Wang, and Z. Wang, "Intuitive control of humanoid soft-robotic hand BCL-13," in *Proc. IEEE-RAS 18th Int. Conf. Humanoid Robots*, Nov. 2018, pp. 314–319.
- [80] Leap Motion Sensor With Orion SDK, by Leap Motion INC. [Online]. Available: <https://www.leapmotion.com>
- [81] D. P. Holland, C. Abah, M. Velasco-Enriquez, M. Herman, G. J. Bennett, E. A. Vela, and C. J. Walsh, "The soft robotics toolkit: Strategies for overcoming obstacles to the wide dissemination of soft-robotic hardware," *IEEE Robot. Autom. Mag.*, vol. 24, no. 1, pp. 57–64, Mar. 2017.
- [82] R. Deimel, M. Radke, and O. Brock, "Mass control of pneumatic soft continuum actuators with commodity components," in *Proc. IEEE/RSJ Int. Conf. Intell. Robots Syst.*, Oct. 2016, pp. 774–779.

- [83] B. Taheri, D. Case, and E. Richer, "Force and stiffness backstepping-sliding mode controller for pneumatic cylinders," *IEEE/ASME Trans. Mechatronics*, vol. 19, no. 6, pp. 1799–1809, Dec. 2014.
- [84] M. van Damme, B. Vanderborght, P. Beyl, R. Versluys, I. Vanderniepen, R. van Ham, P. Cherelle, and F. Daerden, "Sliding mode control of a 'soft' 2-DOF planar pneumatic manipulator," *Int. Appl. Mech.*, vol. 44, no. 10, pp. 1191–1199, Oct. 2008.
- [85] E. J. Barth, J. Zhang, and M. Goldfarb, "Sliding mode approach to PWM-controlled pneumatic systems," in *Proc. Amer. Control Conf.*, May 2002, pp. 2362–2367.
- [86] H. P. H. Anh and N. T. Nam, "A new approach of the online tuning gain scheduling nonlinear PID controller using neural network," in *Proc. IntechOpen*, Apr. 2011, pp. 1–24.
- [87] K. Khayati, P. Bigras, and L.-A. Dessaint, "LuGre model-based friction compensation and positioning control for a pneumatic actuator using multi-objective output-feedback control via LMI optimization," *Mechatronics*, vol. 19, no. 4, pp. 535–547, 2009.
- [88] T. Leephakpreeda, "Fuzzy logic based PWM control and neural controlled-variable estimation of pneumatic artificial muscle actuators," *Expert Syst. Appl.*, vol. 38, no. 6, pp. 7837–7850, Jun. 2011.
- [89] X. Gao and Z.-J. Feng, "Design study of an adaptive Fuzzy-PD controller for pneumatic servo system," *Control Eng. Pract.*, vol. 13, no. 1, pp. 55–65, Jan. 2005.
- [90] J. Zhou, X. Chen, U. Chang, Y. Liu, Y. Chen, and Z. Wang, "A grasping component mapping approach for soft robotic end-effector control," in *Proc. 2nd IEEE Int. Conf. Soft Robot. (RoboSoft)*, Apr. 2019, pp. 650–655.



JUI-TING LU received the Undergraduate Diploma degree from Claude Bernard University Lyon 1 (UCBL), in 2017. She is currently pursuing the master's degree in applied mathematics with UCBL and École Normale Supérie de Lyon, France. She was a Visiting Student with the Bionics and Control Lab, Department of Mechanical Engineering, The University of Hong Kong. Her research interests include the fields of discrete geometric analysis and vector calculus on meshes.



CLARISSE CHING YAU LEUNG is currently pursuing the bachelor's degree with The University of Hong Kong, where she was a Student Research Assistant with the Bionics and Control Lab, Department of Mechanical Engineering. Her research interests include arts and design, automated construction, and robotics in architecture.



YONGHUA CHEN received the B.Sc. degree in mechanical engineering from Southwest Jiaotong University and the Ph.D. degree from the University of Liverpool, U.K.

Before joining The University of Hong Kong as a Lecturer, he was with Motorola Electronics Pte., Ltd., Singapore, Asia Matsushita Electronics Pte., Ltd., Singapore, and Swire Technologies Pte., Ltd., Hong Kong, where he gained extensive experiences in automation, robotics, and engineering an Associate Professor with the Department of Mechanical Engineering, The University of Hong Kong. He has filed five patents, coauthored three books, and published over 230 referred papers in international journals and conferences. His current research interests include soft robotics, exoskeleton, and additive manufacturing.



YONG HU (M'07–SM'11) received the B.Sc. and M.Sc. degrees in biomedical engineering from Tianjin University, Tianjin, China, in 1985 and 1988, respectively, and the Ph.D. degree from The University of Hong Kong, Hong Kong, in 1999, where he is currently an Associate Professor and the Director of the Neural Engineering and Clinical Electrophysiology Laboratory, Department of Orthopaedics and Traumatology. His research interests include neural engineering, clinical electrophysiology, and biomedical signal measurement and processing.



ZHENG WANG (S'06–M'10–SM'16) received the B.Sc. degree (Hons.) in automatic control from Tsinghua University, Beijing, China, in 2004, the M.Sc. degree (Hons.) in control systems from the Imperial College London, London U.K., in 2005, and the Ph.D. degree (Hons.) in electrical engineering from Technische Universität München, Munich, Germany, in 2010. He was a Postdoctoral Research Fellow with Nanyang Technological University, Singapore, from 2010 to 2013, and a Postdoctoral Fellow with the School of Engineering and Applied Sciences and the Wyss Institute of Bioinspired Engineering, Harvard University, in 2013 and 2014, respectively. Since July 2014, he has been an Assistant Professor with the Department of Mechanical Engineering, The University of Hong Kong, Hong Kong. He has been a Professor in robotics with the Department of Mechanical and Energy Engineering, Southern University of Science and Technology, China, since February 2019. His research interests include haptics human–robot interaction, endoscopic surgical robot, underwater robots, and soft robotics.



JIANSHU ZHOU (S'16) received the B.Sc. degree from Central South University, Changsha, China, in 2015, and the M.Sc. degree in mechanical engineering from The University of Hong Kong, Hong Kong, in 2016, where he is currently pursuing the Ph.D. degree in mechanical engineering. His research interests include soft robotics, dexterous and robust grasping, variable stiffness mechanism, and proprioceptive soft actuators.



XIAOJIAO CHEN (S'16) received the B.Eng. degree in mechanical engineering from the Huazhong University of Science and Technology, Wuhan, China, in 2012, and the M.S. degree in mechanical engineering from The University of Hong Kong, Hong Kong, in 2015, where he is currently pursuing the Ph.D. degree in soft robotics.

His research interests include the field of soft actuators, soft robotic arms, variable stiffness control, and human–robot interaction.



UKYOUNG CHANG received the B.Sc. degree in biology from Duke University, in 2016. She pursued as a Research Assistantship with the University of California Davis and the Department of Mechanical Engineering, The University of Hong Kong. Her research interests include ecology, biomechanics, and bioinspired robotics.